Original Article

Accumulated myeloid-derived suppressor cells demonstrate distinct phenotypes and functions in two non-alcoholic steatohepatitis mouse models

Hiromichi Tsunashima[1], Koichi Tsuneyama[2], Yuki Moritoki[3], Masumi Hara[1], Kentaro Kikuchi[1]

[1]Fourth Department of Internal Medicine, Teikyo University Mizonokuchi Hospital, Kawasaki-shi, Kanagawa 213-8507, Japan; [2]Department of Diagnostic Pathology, Graduate School of Medicine and Pharmaceutical Science, University of Toyama, Toyama-shi, Toyama 930-0194, Japan; [3]Department of General Medical Practice and Laboratory Diagnostic Medicine, Akita University Graduate School of Medicine, Akita-shi, Akita 010-8543, Japan

Correspondence to: Dr. Kentaro Kikuchi. The Fourth Department of Internal Medicine, Teikyo University Mizonokuchi Hospital, 3-8-3 Mizonokuchi, Takatsu-ku, Kawasaki-shi, Kanagawa 213-8507, Japan. Email: kentaro@med.teikyo-u.ac.jp.

Background: To examine the steady state of hepatic myeloid-derived suppressor cells (MDSCs) and the lipid accumulation and inflammation-related changes in these cells, we analyzed the presence and functions of hepatic MDSCs in the following two non-alcoholic steatohepatitis (NASH) mouse models.

Methods: Monosodium glutamate (MSG) model; MSG was subcutaneously injected into neonatal male C57BL/6J mice that were fed with normal diet up to 18 weeks of age. Methionine/choline-deficient diet (MCD) model; 16-week-old male C57BL/6J mice were fed with an MCD for 2 weeks. Those hepatic MDSCs were evaluated by flow cytometry and immunohistochemically.

Results: Both MSG and MCD mice exhibited greater numbers of hepatic lipid droplets than 18-week-old male control mice. Hepatocellular ballooning was obvious in MSG, whereas inflammatory cell infiltration were apparent in MCD mice. CD11b, CD115, and Gr-1-positive hepatic MDSCs were increased in both models but higher in MCD mice, and demonstrated higher expression of an M2 macrophage marker CD206 mean fluorescence intensity (MFI) in MSG compared to MCD mice. Degree of reactive oxygen species production was evaluated using the DCFDA MFI values, which were significantly elevated in hepatic MDSCs from MCD mice. MSG mouse livers demonstrated Gr-1 positive cell accumulation around lipid droplets, mimicking crown-like structures in adipose tissues. In contrast, hepatic Gr-1 positive cells were primarily located in inflammatory cell aggregates in MCD mice.

Conclusions: These results suggest that hepatic fatty changes promote MDSC accumulation, and inflammatory changes induce phenotypic and functional alteration in hepatic MDSCs in NASH mouse models.

Keywords: Myeloid-derived suppressor cells (MDSCs); non-alcoholic steatohepatitis (NASH)

Submitted Nov 05, 2014. Accepted for publication Mar 06, 2015.
doi: 10.3978/j.issn.2304-3881.2015.04.08
View this article at: http://dx.doi.org/10.3978/j.issn.2304-3881.2015.04.08

Introduction

Non-alcoholic fatty liver disease (NAFLD) and its advanced stage, non-alcoholic steatohepatitis (NASH), are liver phenotypes of metabolic syndrome that develop from fatty liver based on insulin resistance and "second hits" such as oxidative stress and inflammatory cytokines, and are known to progress to liver cirrhosis and cancer (1).

There is an urgent need to elucidate NASH pathophysiology because NAFLD represents a national health burden in Japan, where the prevalence is 1 of 3 citizens (2) and the 5-year cumulative cancer-causing rate is 20% in NASH cases that progress to liver cirrhosis (3).

Immunological mechanisms such as cytokine production and immunological reactions to oxidative stress appear to be involved in progression of liver pathology; however, the details remain to be clarified.

Myeloid-derived suppressor cells (MDSCs) are involved in the suppression of inflammation and cellular immunity, and also play a major role in anti-cancer immunity (4). There have been few reports on the steady state of hepatic $CD11b^+$ $Gr\text{-}1^+$ MDSCs or on changes in hepatic cells consequent to an inflammatory environment (5). In the present study, we analyzed the histopathological and functional characteristics of hepatic MDSCs in NASH mouse models and examined the influence of MDSCs on NASH pathology.

Methods

Generation of two different NASH mouse models

Monosodium glutamate (MSG) mice

Neonatal male C57BL/6J mice were subcutaneously injected with MSG, as described previously (6). MSG [Sodium hydrogen L(+)-glutamate monohydrate, Wako Pure Chemical Industries Ltd, Osaka, Japan] was dissolved in saline, which solution was injected using 30-gauge needles at a dose of 4 mg/g body weight into the subcutaneous spaces under dorsal skins of six male C57BL/6J mice (Charles River Laboratories Japan Inc., Kanagawa, Japan) during the first 5 days after birth. The mice were fed with a regular diet and housed up to 18 weeks of age under conventional conditions.

Methionine/choline-deficient diet (MCD) mice

Six 16-week-old male C57BL/6J mice were fed with an MCD for 2 weeks and were kept under the same conditions as the MSG group. Six 18-week-old male mice fed with a regular diet were used as the control group.

After the mice were sacrificed by cervical dislocation, ALT levels were measured in serum samples prepared from venous blood. The livers were extracted, fixed in formalin, stained with hematoxylin and eosin (HE), and then evaluated pathologically according to the NAFLD activity score (NAS) (7). The remainders of the livers were used for immunohistochemical staining and cell preparation for flow cytometric analysis. This study was approved by the Teikyo University School of Medicine Animal Ethics Committee (approval number 09-009) and was conducted in accordance with the institutional guidelines.

Flow cytometric analysis

Hepatic mononuclear cells (HMNCs) were isolated as follows. The livers were perfused with phosphate-buffered saline (PBS) containing 0.5% bovine serum albumin (BSA) and 0.04% EDTA (PBS buffer), filtered through a 40-μm cell strainer (BD Falcon, Durham, NC, USA), and resuspended in PBS buffer. The cells were pelleted by centrifugation at 500 rpm for 5 min, and the supernatant was centrifuged again at 1,200 rpm for 5 min. After discarding the supernatant, the precipitate was dissolved in PBS buffer, layered over 1.077 g/mL-density Lymphoprep (Axis-Shield Proc. AS, Oslo, Norway), and centrifuged at 1,400 rpm for 15 min to isolate HMNCs by the density gradient method. The HMNC layer was then collected and washed with PBS buffer. Viable cells were counted by trypan blue staining.

For cell surface staining, 1×10^6 HMNCs in a 1.5-mL tube were initially subjected to Fc receptor blocking at 4 ℃ for 10 min with a solution prepared by dissolving 1 μL of purified anti-mouse CD16/32 (BioLegend, San Diego, CA, USA) in 24 μL of cell staining buffer (BioLegend). Subsequently, the cells were incubated at 4 ℃ for 15 min under a dark condition in a 25 μL solution containing cell staining buffer and appropriate quantities of Alexa Fluor 488-conjugated anti-mouse Gr-1 (BioLegend), phycoerythrin (PE)-conjugated anti-mouse F4/80, CD36, CD206 (BioLegend), PE-conjugated rat IgG2a-kappa isotype control (BioLegend), allophycocyanin (APC)/Alexa Fluor 750-conjugated anti-mouse CD11b (BioLegend), or APC-conjugated anti-mouse CD115 (BioLegend). After washing, the total volume was adjusted to 200 μL with PBS buffer, and the cells were dispensed into a 96-well round-bottom plate. Flow cytometric analysis was performed on a BD FACSArray flow cytometer (BD Immunocytometry Systems, San Jose, CA, USA) with FACSArray software (BD Immunocytometry Systems).

Detection of reactive oxygen species

Initially, 1×10^6 HMNCs were placed in a 1.5-mL tube and suspended in 500 μL of RPMI, next, 2.5 μM of chloromethyl derivative of 2',7'-dichlorodihydrofluorescein diacetate (CM-H_2DCFDA, Molecular Probes, Eugene, OR, USA) was added and the preparation was incubated at 37 ℃ for 30 min. After washing with PBS, appropriate amounts of PE-conjugated anti-mouse Gr-1, APC/Alexa Fluor 750-conjugated anti-mouse CD11b and APC-conjugated

anti-mouse CD115 (BioLegend) were added along with cell staining buffer to achieve a final solution volume of 25 μL. The cell suspension was subsequently incubated in a dark room at 4 ℃ for 15 min. After washing with PBS, the cells were prepared and analyzed by flow cytometry; the DCFDA mean fluorescence intensity (MFI) values were compared to those of the isotype control.

Immunohistochemical staining

According to an immunoenzymatic method, the formalin-fixed tissue slices were subjected to deparaffinization, a 15-min heat treatment in a microwave for antigen retrieval, gradual cooling, and endogenous peroxidase was blocked using H_2O_2 containing tris-buffered saline (TBS). After blocking non-specific reaction using TBS containing 5% BSA, overnight incubation was carried out with ×100 primary antibodies of rabbit polyclonal anti-mouse Gr-1 (Bioss Inc., Boston, USA) and rabbit polyclonal anti-mouse myeloperoxidase (Dako, Glostrup, Denmark). After washing with TBS-tween, following incubation with peroxidase-conjugated immunepolymer for rabbit polyclonal antibodies (Envison-PO for rabbit, Dako, Glostrup, Denmark) as secondary antibody at room temperature for 1 hour. After washing with TBS, 3,3'-diaminobenzidine was used for color development. Hematoxylin was used as nuclear counterstaining.

Statistical analysis

Serum ALT, NAS, MDSC frequency, calculated number of MDSC per gram of liver and CD36, CD206, and DCFDA MFI ratios (sample MFI divided by isotype control MFI) are presented as mean ± standard error of measurement (SEM). Statistical analysis was performed with the non-parametric Mann-Whitney test or Kruskal-Wallis analysis of variance using Statview version 5.0 software for Macintosh (SAS institute Inc., Cary, NC, USA), and differences were considered significant when $P<0.05$.

Results

Characteristics of the two different NASH mouse models

Large numbers of lipid droplets were observed in the livers of both MSG and MCD mice. Strong inflammatory cell infiltrations were observed in MCD mice, but were mild and faint respectively in MSG mice (*Figure 1A*). Serum ALT levels increased significantly in both MSG (41.3±2.3 IU/L) and MCD (54.2±5.8 IU/L) mice compared to those in control mice (18.6±1.3 IU/L, $P<0.001$) (*Figure 1B*). Inflammation and fibrosis scores were significantly higher in MCD mice, whereas hepatocellular ballooning was significantly more severe in MSG mice.

Frequencies and characteristics of hepatic MDSCs

Mouse hepatic MDSCs were positive for CD11b, CD115 and Gr-1 (*Figure 2A*). In the CD11b and CD115-positive cell population, the ratios of MDSCs, which are Gr-1-positive, were significantly higher in MSG (68.3%±2.5%) and MCD (76.1%±1.7%) mice (compared to control mice, 43.2%±5.5%, $P<0.001$). Furthermore, the counts for these cells were also significantly high when converted to per gram of liver for both MSG and MCD mice and higher in MCD mice (*Figure 2B*). MDSCs were negative for F4/80, and CD36 MFI ratios were significantly higher in both MSG and MCD mice compared to control mice, however, no significant difference was observed between the two NASH mouse models. In contrast, the CD206 MFI ratio was significantly higher in MSG mice (10.4±0.3, *vs.* MCD mice: 9.1±0.3, $P=0.001$, *vs.* control mice: 7.6±0.3, $P=0.0009$), whereas the DCFDA MFI ratio was significantly higher in MCD mice (4.5±0.3, *vs.* MSG mice: 3.3±0.5, $P=0.01$, *vs.* control mice: 2.6±0.4, $P=0.0008$).

Gr-1 staining in the liver

Large numbers of Gr-1-positive cells were observed in the livers of MSG and MCD mice. In contrast, the control livers demonstrated only a small number of Gr-1-positive cells in the parenchyma (*Figure 3*). These cells were round, mononucleated and most of the cells were myeloperoxidase-negative (data not shown). Images of the MSG-treated mice revealed that the Gr-1-positive cells were localized around lipid droplets and demonstrated similar form to crown-like structures. In MCD mice, Gr-1 positive cells were distributed in inflammatory cell aggregates.

Discussion

To clarify the characteristic difference of MDSCs in between steatosis and inflammation, we used MSG and MCD. When MSG is administered subcutaneously to neonatal mice, the hypothalamic arcuate nucleus-paraventricular nucleus pathway is compromised, resulting in obesity and

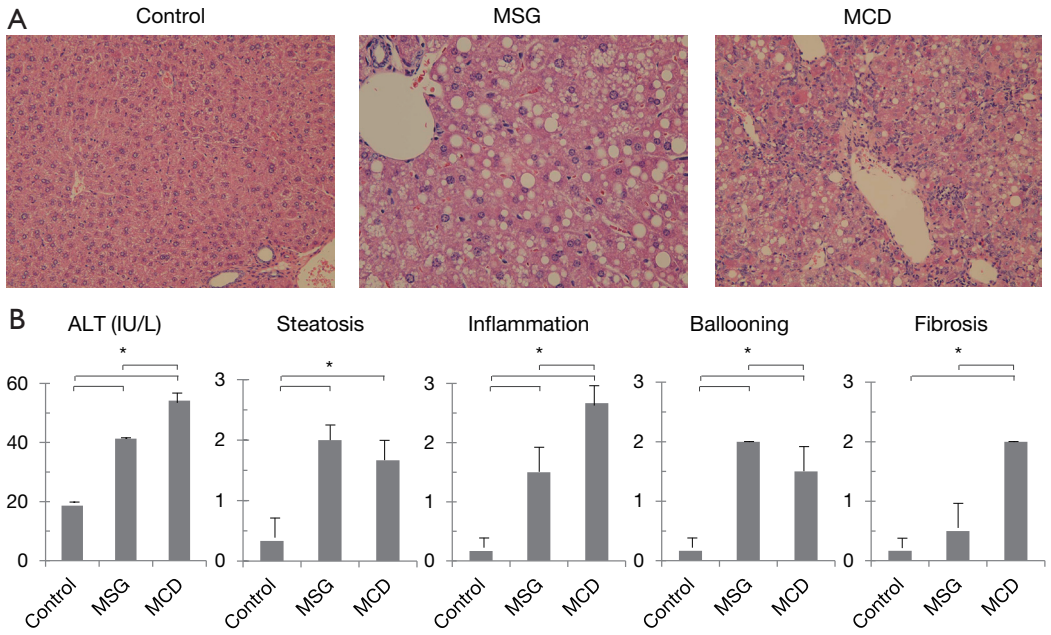

Figure 1 Characteristics of MSG and MCD mice. (A) Histopathological images of the livers (hematoxylin-eosin staining, 200×). A representative result from each mouse model is shown; (B) comparison of serum ALT levels and NAFLD activity scores (NASs). The mean values ± standard errors of measurement are shown for six mice per group (P<0.05). MSG, monosodium glutamate; MCD, methionine/choline-deficient diet; NAFLD, non-alcoholic fatty liver disease.

hyperleptinemia, even in mice fed with a normal diet (8). In MSG-treated mouse livers, severe steatosis and mild inflammatory cell infiltration occur as a function of age, and these features are similar to those of human NAFLD/NASH (9-12). As another NASH model, it is well known that MCD feeding rapidly induces mild steatosis and considerably severe inflammation in the livers because of VLDL synthetic obstacle (13).

To compare the state of MDSCs in the distinct levels of steatosis and inflammation in the liver, two NASH mouse models were prepared herein using injected MSG or MCD to C57BL/6J mice. In both mouse models, large numbers of lipid droplets were observed in the livers. In addition, severe hepatocellular ballooning was observed in MSG mice, whereas severe inflammatory cell infiltration and fibrosis were observed in MCD mice. Flow cytometric analysis revealed significantly increased numbers of hepatic MDSCs were observed in MSG and MCD mice but higher in MCD mice. We found MDSCs were increased according to inflammatory grade in the liver of NASH mouse models. To date, no study has evaluated MDSCs in NAFLD and NASH; therefore, this is the first report to clarify increment of hepatic MDSCs in NASH mouse models. Subsequently, we examined whether differences in the MDSC phenotypes or functions existed between the two mouse models that represented different degrees of hepatic inflammation. Although no differences in CD36 expression were detected, the CD206 MFI ratio was higher in MSG mice, whereas the DCFDA MFI ratio was higher in MCD mice. Based on these results, we believe that MDSCs may undergo transition from an M2 to an M1 phenotype as inflammation progresses (14,15).

Pathological analysis also showed an increased number of Gr-1-positive MDSCs in the MSG and MCD mice. Some part of Gr-1 positive cells aggregated around fat vacuoles and mimicked crown-like structures in adipose tissue. Meanwhile, localization differed in MCD mice such that Gr-1 positive cells were observed within the inflammatory cell aggregates.

In this study, we found in MSG mice, MDSCs are involved in lipid metabolism in a manner similar to that of M2 macrophages; in contrast, in MCD mice, MDSCs are believed to be involved in inflammation control (16-18). In an earlier experiment, we examined IL-10 production

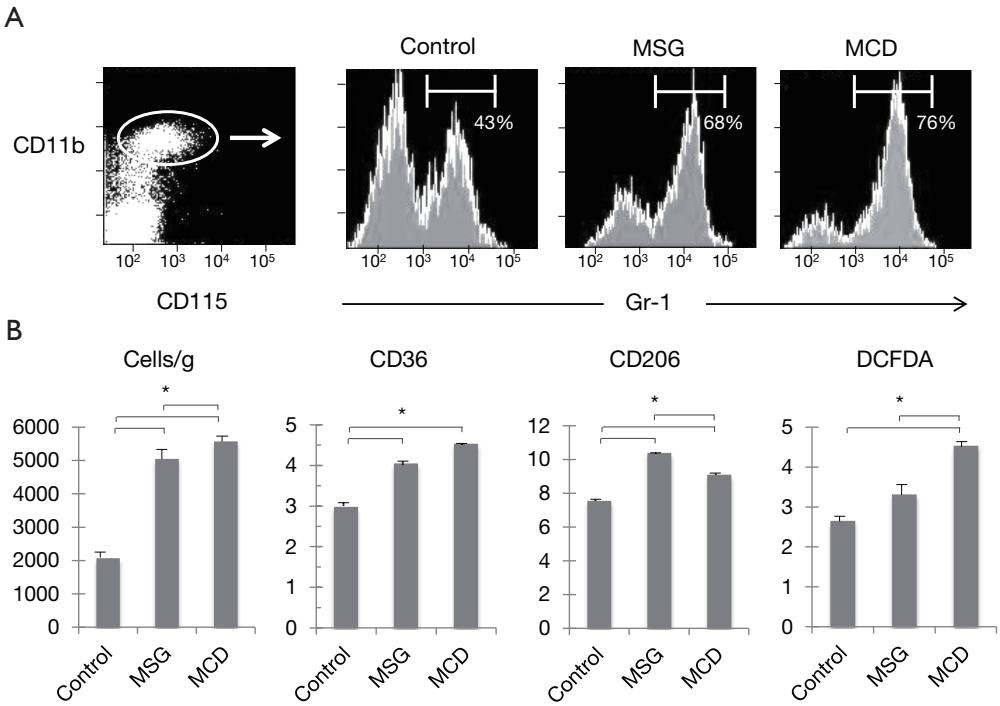

Figure 2 Phenotyping and quantification of myeloid-derived suppressor cells (MDSCs) from the livers of MSG and MCD mice and reactive oxygen species production. (A) MDSC (Gr-1-positive) frequencies among CD11b and CD115-positive cell aggregates. A representative flow cytometric analysis plot is shown for each condition; (B) a comparison of CD36, CD206, and DCFDA MFI ratios and the numbers of MDSCs per gram of liver. The mean values ± standard errors of measurement are shown for 6 mice per group (P<0.05). MSG, monosodium glutamate; MCD, methionine/choline-deficient diet; MFI, mean fluorescence intensity.

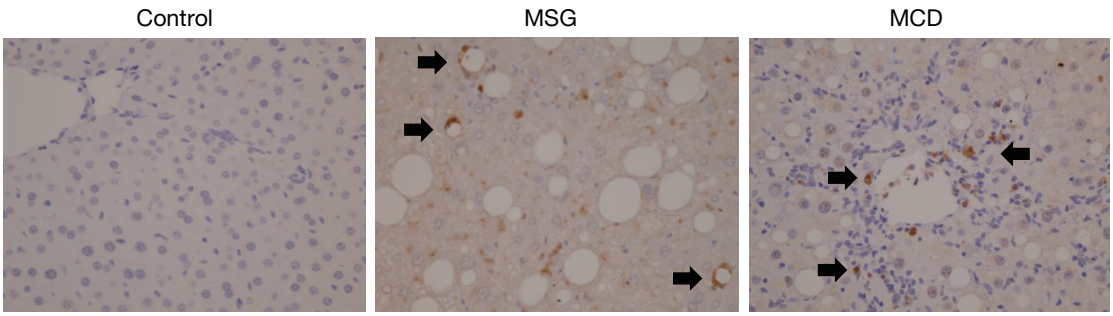

Figure 3 Gr-1 staining of the livers from MSG and MCD mice. Gr-1-positive cells are indicated by an arrow (400×). One representative result is shown for each condition. MSG, monosodium glutamate; MCD, methionine/choline-deficient diet.

in MDSCs from the livers of MSG and MCD mice in response to lipopolysaccharide stimulation. Although MDSCs from both models produced IL-10, levels of which were comparable difference in the amount of IL-10 produced (unpublished data).

The underlying mechanism behind cancer development in NASH remains unknown. Although we could not examine carcinogenesis in the present study, MDSCs control tumor immunity via IL-10 and arginase (19), the increased numbers of MDSCs observed in NASH may be

involved in cancer development and progression. In recent years, MDSC suppression, which is under investigation as an anti-cancer therapy (20), and this may represent a potential for a novel treatment for NASH.

In conclusion, we demonstrated that the number of MDSCs increased in accordance with lipid accumulation and inflammatory changes in the livers of the NASH model mice suggesting that MDSCs play a significant role in immunometabolism.

Acknowledgements

The authors would like to thank Dr. Munehiro Honda (Mishuku Hospital, Meguro, Tokyo, Japan) for the outstanding flow cytometric assistance, Dr. Hiroshi Miyakawa (Teikyo University Mizonokuchi Hospital, Kanagawa, Japan) for his expertise in this study.
Funding: This work was supported by a Grant from the Ministry of Health, Labour and Welfare of Japan and JSPS KAKENHI Grant-in-Aid for Scientific Research (C) Number 24590952 and (B) Number 24390181.

Footnote

Conflicts of Interest: The authors have no conflicts of interest to declare.

Ethical Statement: This study was approved by the Teikyo University School of Medicine Animal Ethics Committee (approval number 09-009) and was conducted in accordance with the institutional guidelines.

References

1. Shimada M, Hashimoto E, Taniai M, et al. Hepatocellular carcinoma in patients with non-alcoholic steatohepatitis. J Hepatol 2002;37:154-60.
2. Omagari K, Morikawa S, Nagaoka S, et al. Predictive factors for the development or regression of Fatty liver in Japanese adults. J Clin Biochem Nutr 2009;45:56-67.
3. Hashimoto E, Yatsuji S, Kaneda H, et al. The characteristics and natural history of Japanese patients with nonalcoholic fatty liver disease. Hepatol Res 2005;33:72-6.
4. Ostrand-Rosenberg S, Sinha P. Myeloid-derived suppressor cells: linking inflammation and cancer. J Immunol 2009;182:4499-506.
5. Chen S, Akbar SM, Abe M, et al. Immunosuppressive functions of hepatic myeloid-derived suppressor cells of normal mice and in a murine model of chronic hepatitis B virus. Clin Exp Immunol 2011;166:134-42.
6. Nakanishi Y, Tsuneyama K, Fujimoto M, et al. Monosodium glutamate (MSG): a villain and promoter of liver inflammation and dysplasia. J Autoimmun 2008;30:42-50.
7. Kleiner DE, Brunt EM, Van Natta M, et al. Design and validation of a histological scoring system for nonalcoholic fatty liver disease. Hepatology 2005;41:1313-21.
8. Olney JW. Brain lesions, obesity, and other disturbances in mice treated with monosodium glutamate. Science 1969;164:719-21.
9. Yamazaki Y, Usui I, Kanatani Y, et al. Treatment with SRT1720, a SIRT1 activator, ameliorates fatty liver with reduced expression of lipogenic enzymes in MSG mice. Am J Physiol Endocrinol Metab 2009;297:E1179-86.
10. Collison KS, Maqbool ZM, Inglis AL, et al. Effect of dietary monosodium glutamate on HFCS-induced hepatic steatosis: expression profiles in the liver and visceral fat. Obesity (Silver Spring) 2010;18:1122-34.
11. Sasaki Y, Shimada T, Iizuka S, et al. Effects of bezafibrate in nonalcoholic steatohepatitis model mice with monosodium glutamate-induced metabolic syndrome. Eur J Pharmacol 2011;662:1-8.
12. Fujimoto M, Tsuneyama K, Fujimoto T, et al. Spirulina improves non-alcoholic steatohepatitis, visceral fat macrophage aggregation, and serum leptin in a mouse model of metabolic syndrome. Dig Liver Dis 2012;44:767-74.
13. Larter CZ, Yeh MM. Animal models of NASH: getting both pathology and metabolic context right. J Gastroenterol Hepatol 2008;23:1635-48.
14. Umemura N, Saio M, Suwa T, et al. Tumor-infiltrating myeloid-derived suppressor cells are pleiotropic-inflamed monocytes/macrophages that bear M1- and M2-type characteristics. J Leukoc Biol 2008;83:1136-44.
15. Yang WC, Ma G, Chen SH, et al. Polarization and reprogramming of myeloid-derived suppressor cells. J Mol Cell Biol 2013;5:207-9.
16. Shaul ME, Bennett G, Strissel KJ, et al. Dynamic, M2-like remodeling phenotypes of CD11c+ adipose tissue macrophages during high-fat diet--induced obesity in mice. Diabetes 2010;59:1171-81.
17. Fujisaka S, Usui I, Bukhari A, et al. Regulatory mechanisms for adipose tissue M1 and M2 macrophages in

diet-induced obese mice. Diabetes 2009;58:2574-82.
18. Sinha P, Clements VK, Bunt SK, et al. Cross-talk between myeloid-derived suppressor cells and macrophages subverts tumor immunity toward a type 2 response. J Immunol 2007;179:977-83.
19. Yang L, DeBusk LM, Fukuda K, et al. Expansion of myeloid immune suppressor Gr+CD11b+ cells in tumor-bearing host directly promotes tumor angiogenesis. Cancer Cell 2004;6:409-21.
20. Apetoh L, Végran F, Ladoire S, et al. Restoration of antitumor immunity through selective inhibition of myeloid derived suppressor cells by anticancer therapies. Curr Mol Med 2011;11:365-72.

Cite this article as: Tsunashima H, Tsuneyama K, Moritoki Y, Hara M, Kikuchi K. Accumulated myeloid-derived suppressor cells demonstrate distinct phenotypes and functions in two non-alcoholic steatohepatitis mouse models. HepatoBiliary Surg Nutr 2015;4(5):313-319. doi: 10.3978/j.issn.2304-3881.2015.04.08

